

# Germline expression of H-Ras<sup>G12V</sup> causes neurological deficits associated to Costello syndrome

J. Viosca<sup>†,1</sup>, A. J. Schuhmacher<sup>†,1</sup>, C. Guerra<sup>‡,\*</sup>  
and A. Barco<sup>†,\*</sup>

<sup>†</sup>Instituto de Neurociencias de Alicante (Universidad Miguel Hernández-Consejo Superior de Investigaciones Científicas), Campus de Sant Joan, Apt. 18, Sant Joan d'Alacant, 03550 Alicante, Spain, and <sup>‡</sup>Molecular Oncology Programme, Centro Nacional de Investigaciones Oncológicas (CNIO), E-28029 Madrid, Spain

\*Corresponding authors: A. Barco, Instituto de Neurociencias de Alicante (UMH-CSIC), Campus de Sant Joan, Apt. 18, Sant Joan d'Alacant 03550, Alicante, Spain. E-mail: abarco@umh.es; C. Guerra, Centro Nacional de Investigaciones Oncológicas (CNIO), E-28029 Madrid, Spain. E-mail: cguerra@cnio.es

**Costello syndrome (CS) is a rare congenital disorder caused by germline activation of H-Ras oncogenes. A mouse model of CS generated by introduction of an oncogenic Gly12Val mutation in the mouse H-Ras locus using homologous recombination in embryonic stem (ES) cells has been recently described. These mice phenocopied some of the abnormalities observed in patients with CS, including facial dysmorphism and cardiomyopathies. We investigated here their neurological and behavioral phenotype. The analysis of H-Ras<sup>G12V</sup> mice revealed phenotypes that resembled the hypermotivity, hypersensibility and cognitive impairments observed in children with CS. Stronger neurological deficits were found in the analysis of mice homozygous for this mutation than in the analysis of heterozygous mice, suggesting the existence of a gene dose effect. These mice represent the first mouse model for CS, offering an experimental tool to study the molecular and physiological alterations underlying the neurological manifestations of CS and to test new therapies aimed at preventing or ameliorating the cognitive and emotional impairments associated to this condition.**

Keywords: Anxiety, Costello syndrome, H-Ras, mental retardation, mouse model

Received 2 July 2008, accepted for publication 14 September 2008

Costello syndrome (CS) is a rare congenital disorder comprising developmental delay, craniofacial anomalies, mental retardation, certain predisposition to tumor development and charac-

teristic cardiac and skeletal problems (Costello 1971; Hennekam 2003; Rauen *et al.* 2008). CS belongs to a group of neuro-cardio-facio-cutaneous (NCFC) developmental syndromes that shares a number of phenotypic traits and includes familial Neurofibromatosis type 1, LEOPARD syndrome, Noonan syndrome and cardio-facio-cutaneous syndrome. Although there is significant overlap in their clinical manifestations, the recent discovery that NCFC syndromes result from *de novo* germline activating mutations in different components of the RAS/RAF/MEK signaling pathway now allows for precise differential molecular diagnosis of these disorders (Aoki *et al.* 2008, Schubbert *et al.* 2007a, 2007b). Each syndrome is characterized by mutations in specific loci. Most CS patients carry activating mutations in H-Ras (Aoki *et al.* 2005; Bertola *et al.* 2007; Estep *et al.* 2006; Gripp *et al.* 2006; Kerr *et al.* 2006; Zenker *et al.* 2007). RAS/RAF/MEK signaling is involved in various critical processes in the nervous systems. In particular, the activation of this signaling cascade has been critically involved in cognitive and emotional processes, including anxiety, depression, addiction and learning and memory (Barco *et al.* 2006; Lonze & Ginty 2002; Thomas & Haganir 2004). It is therefore not surprising that abnormal signaling in this pathway led to multiple neurological manifestations in CS patients.

The neurological study of patients suffering from CS have revealed that mental retardation is, in general, not severe ranking from mild to borderline mental impairment (Axelrad *et al.* 2004, 2007). Longitudinal analyses revealed that cognitive abilities were stable, without progressive deterioration, and there was significant improvement in daily living skills and adaptive behavior (Axelrad *et al.* 2007). Children with CS have increased difficulty with anxiety and higher irritability, manifested in hypersensitivity to sound and tactile stimuli, sleep disturbance and excess shyness (Galera *et al.* 2006; Kawame *et al.* 2003). Contrary to prior suggestions, a recent longitudinal study showed that the difficulty of internalizing and externalizing problems was comparable across the age range and did not decline with aging (Axelrad *et al.* 2007).

A strain of genetically modified mice carrying a point mutation in the H-Ras locus previously associated to CS, the substitution of Gly12 by Val, was generated to better understand the developmental and physiological defects associated to this disorder. These mice were viable and displayed many of the phenotypic abnormalities observed in CS patients, such as de facial dysmorphism and cardiomyopathies (Schuhmacher *et al.* 2008). We carried out here a comprehensive behavioral analysis of H-Ras<sup>G12V</sup> mice to evaluate the suitability of this mutant strain for modeling the neurological and behavioral alterations observed in CS patients. We found that H-Ras<sup>G12V</sup> mice exhibit phenotypes that resemble the hypermotivity, hypersensibility and cognitive impairments observed in children with CS. The neurological deficits

<sup>1</sup>These two authors contributed equally to this work.

were especially strong in mice homozygous for this mutation, suggesting a possible gene dose effect. This mutant mouse strain represents a useful tool to study the molecular and physiological alterations underlying the neurological manifestations of CS and to test new therapies aimed at preventing or ameliorating those impairments.

## Materials and methods

### Targeted mutation of H-Ras locus

H-*Ras*<sup>geo/geo</sup>, H-*Ras*<sup>+G12V</sup> and H-*Ras*<sup>G12V/G12V</sup> knock-in mice have been described before (Schuhmacher *et al.* 2008). Briefly, homologous recombinants R1 ES clones carrying the modifications at the H-*Ras* locus (H-*Ras*<sup>geo</sup> and H-*Ras*<sup>LSLG12V</sup> alleles described on Supplemental Fig. S1) were used to generate chimeric mice by microinjection into C57BL/6J blastocysts. These mice were crossed to C57BL/6J females to obtain germline transmission of the targeted alleles. Generation of mice carrying the H-*Ras*<sup>G12V</sup> allele was performed by crossing the H-*Ras*<sup>+LSLG12V</sup> mice with *EllaCre* transgenics (in a C57BL/6J genetic background) that express Cre at the zygote stage, allowing efficient cleavage of the LSL cassette in the germline. Mice carrying the H-*Ras*<sup>G12V</sup> allele were backcrossed for two generations to C57BL/6J mice to eliminate the *EllaCre* transgene and to enrich the C57BL/6J genetic background of the mice. H-*Ras*<sup>+G12V</sup> mice in a C57BL/6J F3 generation were crossed among themselves to generate homozygous mice (H-*Ras*<sup>G12V/G12V</sup>). For the studies described here, H-*Ras*<sup>+G12V</sup>, H-*Ras*<sup>G12V/G12V</sup> and H-*Ras*<sup>+/+</sup> mice were littermates obtained from crosses between H-*Ras*<sup>+G12V</sup> mice. Routine genotyping of H-*Ras*<sup>+</sup>, H-*Ras*<sup>geo</sup>, H-*Ras*<sup>LSLG12V</sup> and H-*Ras*<sup>G12V</sup> alleles was carried out by PCR amplification (Schuhmacher *et al.* 2008). H-*Ras*<sup>+G12V</sup> and H-*Ras*<sup>G12V/G12V</sup> mutant mice, were born at the expected Mendelian ratio, were fertile and survived at comparable rates to their wild-type counterparts for more than 18 months. H-*Ras*<sup>+geo</sup> and H-*Ras*<sup>geo/geo</sup> mice expressing the Geo protein from a nonmutated H-*Ras* allele were also fertile and survived at comparable rates to their wild-type counterparts. Mice were maintained according to animal care standards established by the European Union, group housed in single-sex cages on a light:dark cycle (12/12 h) with food and water available *ad libitum*.

### Histological techniques

For  $\beta$ -galactosidase expression in the adult brain, H-*Ras*<sup>geo/geo</sup> and H-*Ras*<sup>G12Vgeo/G12Vgeo</sup> mice were anesthetized with ketamine/xylazine, perfused and postfixed overnight with 2% paraformaldehyde, and sectioned with a vibratome (50  $\mu$ m sections). Sections were washed twice with phosphate-buffered saline (PBS) and submerged in a staining solution consisting on 5 mM potassium hexacyanoferrate (II), 5 mM Potassium hexacyanoferrate (III), 2 mM MgCl<sub>2</sub> and 1 mg/ml of X-gal (dimethyl sulfoxide) dissolved in PBS. Immunostainings were performed as previously described (Lopez de Armentia *et al.* 2007). Anti-phospho-CREB (Ser133) and anti-phospho-Erk1/2 (Phospho-p44/42 MAPK Thr202/Tyr204 20G11) antibodies were obtained from Cell Signaling Technology (Beverly, MA, USA). Anti-c-fos (Ab-2) was obtained from Calbiochem (La Jolla, CA, USA), and anti-Synaptophysin (clone SVP-38), anti-MAP-2 (clone HM-2) and secondary antibodies were obtained from Sigma Aldrich Quimica S.A. (Madrid, Spain).

### Behavioral studies

Behavioral studies were performed with adult mutant mice and control littermates. Three cohorts of mice were used in our behavioral experiments: Group A: A group of 2-month-old male H-*Ras*<sup>+G12V</sup> mice and wild-type littermates was tested in a battery of tests in the following order: Open Field, Elevated plus maze, modified SHIRPA screen, Rotarod, Novel Object Recognition, Morris water maze (MWM) and Contextual Fear conditioning. Group B: To investigate

further the sensory and exploratory phenotype of heterozygous mice we examined a second cohort of 2-month-old male H-*Ras*<sup>+G12V</sup> mice and wild-type littermates in the following tests: *IntelliCage*, acoustic startle reflex, prepulse inhibition (PPI) and hot plate. Group C: Finally, a cohort of 2- to 3-month-old H-*Ras*<sup>G12V/G12V</sup> mice and wild-type littermates was examined in the same battery of test used for group A plus the hot plate and the *IntelliCage* tests. The group of homozygous mice included both males and females (balanced between genotypes). All behavioral procedures were conducted during the light phase of the light cycle. Experimenter was blind to genotypes. The result of the PCR-based genotyping was provided as a factor for statistical analysis of the behavioral data once the battery of tasks was concluded.

### Modified SHIRPA primary screen

Mice were tested using a modification of Irwin procedure (Irwin 1968). The examination of each animal started with the observation of undisturbed behavior in a cylindrical clear acrylic glass viewing jar (10  $\times$  20 cm). The animal was then transferred to an arena (38  $\times$  20  $\times$  15 cm) for assessment of motor behavior. Next, we conducted a sequence of manipulations to evaluate trunk curl, limb grasping, visual acuity, grip strength, toe pinch response, corneal reflex and pinna reflex. Subsequently, animals were laid on supine restraint for the assessment of vibrissae and the autonomic response of skin color. Limb and abdominal tone, lacrimation, provoked biting and body length were also recorded. The primary screen was completed with the assessment of wire maneuver, righting reflexes, negative geotaxis and weight measurement. Throughout this procedure, incidences of abnormal behavior, fear, irritability, aggression or vocalization were recorded. Additional details are available at <http://www.har.mrc.ac.uk/mousebook/?by=protocols>.

### Open field

Mice were placed in 48  $\times$  48  $\times$  30 cm white acrylic glass boxes (170 lux on the floor of the testing arena) and monitored throughout the test session (30 min) using a videotracking system (SMART, Panlab S.L., Barcelona, Spain) that recorded the position of the animal every 0.5 s. The same software provided measures of traveled distance, resting time (defined as the time that the animal moved with a speed lower than 5 cm/s), maximum speed, average speed (calculated after elimination of resting time), and time spent in the center of the arena.

### IntelliCage

Mice were implanted subcutaneously with a transponder and housed in the *IntelliCage* automated system (NewBehavior AG, Zurich, Switzerland) with all the doors open for 3 days (four to five animals per cage) to evaluate home-cage activity (Galsworthy *et al.* 2005). This equipment records the visits of individual mice to each one of the four corners of a large cage, in which the animals are housed, by means of antennae that recognize the transponders implanted under their skin. The mice have to visit these corners to gain access to water. Corner visits were recorded for each mouse and plotted in blocks of 12 h corresponding to the light and dark phases of the daily light cycle.

### Elevated plus maze

The plus maze made of black acrylic glass consisted of two open arms (50  $\times$  10 cm) and two enclosed arms (50  $\times$  10  $\times$  30 cm) extending from a central platform (10  $\times$  10 cm). The arms were elevated to a height of 50 cm above the floor. The open arms lacked any wall or rims. Indirect halogen illumination provided 210 lux onto the open arms and 45 lux onto the closed arms. Mice were placed in the center of the maze facing a closed arm, and their behavior was recorded for 5 min with a camera located above the maze. The percentage of time spent and number of entries in the different compartments (closed and open arms) were assessed.

### Hot plate

The mouse was placed in the test chamber of a hot plate (Panlab S.L.) set at 52.5°C and the latency until it exhibited heat pain behavior was recorded.

### Acoustic startle response

Animals were placed in restrainers within startle chambers (Panlab S.L.) where a high-frequency speaker produced the acoustic stimuli. A piezoelectric accelerometer mounted under each chamber detected and transduced animal movements. Ten repetitions of 10 different trial types were presented during a test session: 40-ms, 8000-Hz sound pulses of 70, 74, 78, 82, 86, 90, 100, 110 and 120 dB, plus no-stimulus trial (65 dB background noise) were randomly presented with 45-s intertrial interval. The maximal amplitude of movement-transduced signal during a one second time window after the delivery of the stimulus was considered the startle response. For each animal, the response to the different sound intensities was averaged and then subtracted to the background noise response.

### PPI of the startle reflex

For PPI tests, 10 repetitions of eight different trial types were randomly presented with 45-s ITI during a single test session: a 40-ms broadband 120 dB burst (P: pulse-alone trial); three different 20-ms prepulse (pp) trials of 70 dB (pp70), 80 dB (pp80) and 90 dB (pp90); three prepulse-pulse (ppP) trials in which the prepulse stimuli preceded 100 ms the 120 dB pulse; and a no-stimulus trial in which only the background noise was presented. PPI was calculated as the averaged startle magnitude on pulse-alone trials (P), minus the averaged startle magnitude on ppP trials, all divided by the averaged pulse-alone values (% PPI =  $100 \times [(P - ppP)/P]$ ).

### Rotarod

Mice were first trained on a Rotarod (Panlab S.L.) at a constant speed (~15 r.p.m.). They received three trials per day for 2 days. Using this protocol a steady level of performance was attained in both genotypes. On testing day, the Rotarod was set to increase from 4 to 40 r.p.m. over 300 s and the latency to fall was measured.

### Novel object recognition memory task

This task was performed as previously described (Bourtchouladze *et al.* 2003). Mice were habituated to a white acrylic glass open field box for two consecutive days (30 min/day). The third day (training), the mice were allowed to explore for 15 min two objects located at opposite corners of the box (10 cm from walls). The objects were made of small pieces of acrylic glass and metal ensemble together; in average they were 5 × 5 × 5 cm in size and had heterogeneous shapes with salient parts and holes for mouse nose poking. For testing, the animals were presented to one of the training objects and a novel one 24 h after training and were allowed to explore for 15 additional minutes. The familiar and the novel objects differed in shape, color and smell, and were located in the same positions in which the objects were located during the training session. We thoroughly cleaned the objects after use with 70% ethanol or with a commercial cleaning liquid specific for each type of object. In preliminary experiments with C57BL/6J mice, we tested that the mice did not express a preference or aversion for a given object or smell. The use of different objects as novel or familiar, as well as the relative position of the novel object was balanced between genotypes. Time spent exploring the objects both in the training and the testing sessions was measured. The discrimination index (DI) was determined using the following formula:  $DI = 100 \times (\text{Time exploring A} - \text{Time exploring B}) / (\text{Time exploring A} + \text{Time exploring B})$ .

### Morris water maze

The task was performed as previously described (Malleret *et al.* 1999) with minor modifications. We used SMART videotracking software (Panlab S.L.) to track the mouse trajectory in a tank of 170 cm of diameter containing water made opaque with white non-toxic paint (Jovi S.L., Barcelona, Spain). Mice received four trials of 120 s maximum, separated by a 45- to 60-min intertrial interval every day. Mice failing to find the platform after 120 s were gently guided to it by hand and allowed to remain on it for 15 s. The experiment was divided in three phases: V1-V3: 3 days of visible platform task, H1-H8: 8 days of hidden platform task, and R1-R5: 5 days of transfer or reversal task in which the hidden platform was moved to the opposite corner. During the visible platform task the transparent platform was sub-

merged 1 cm under the water and cued with a black bar. The location of the platform changed every trial. In the hidden platform and transfer tasks, the transparent submerged platform was not cued and the location of the platform remained the same during the duration of the task. Probe trials in which the platform was removed were performed on days H5 (P1) and H9 (P2) of the hidden platform task and day R6 (P3) of the transfer task to assess memory formation. For the analysis of probe trials, we calculated quadrant occupancy (% of time), number of crossings in an annulus (area double than platform) located at platform position (TQ, target quadrant), and the average of crossings in same sized annuli at equivalent positions in the other three quadrants of the pool (non-TQ, non-target quadrants).

### Contextual fear conditioning

On training day the mice were placed in the conditioning chamber (Panlab S.L.) for 2 min 28 s and then received a 2-s electric foot shock (0.4 mA for H-*Ras*<sup>+/G12V</sup> mice and littermates and 0.7 mA for H-*Ras*<sup>G12V/G12V</sup> mice and littermates). After an additional 30 s in the chamber, mice were returned to their home cage. Conditioning was assessed 24 h and 1 week later in the same context in which mice were trained by scoring freezing behavior using a piezoelectric accelerometer that transduced animal movements. The software (Freezing from Panlab S.L.) was configured to consider a freezing episode an interval longer than 2 s in which the signal remained below an arbitrary threshold. This threshold was determined using wild-type preconditioned mice.

### Statistical analyses

Statistical analyses used Mann–Whitney tests, *t*-tests and ANOVAS. Type III sum of squares was used in the ANOVA models. Sex was introduced as an additional between-subject factor in the analysis of homozygous mice to determine whether genotype effects were sex dependent. As there was no significant genotype-sex interaction, these results are not reported in the text, the table and the figures. In the case of heterozygous mice this distinction was not necessary because all individuals were male. For this reason in the analysis of some parameters, we used *t*-test in the case of heterozygous mice and littermates and ANOVA in the case of homozygous mice and littermates. Statistical analyses were done using SPSS 12.0 software (Chicago, IL, USA). An alpha value of  $P < 0.05$  was considered statistically significant, whereas analyses in which  $P > 0.05$  were referred as non significant (ns). Means ± SEM or median followed by the interquartile range in parenthesis are presented in the figures and the table.

## Results

### Brain expression of H-*Ras* alleles

The pattern of expression in the brain of wild-type and mutant H-*Ras* alleles can be easily examined using the knock-in mouse strains generated by Schuhmacher *et al.* (2008). To monitor H-*Ras* expression at the single cell level, an IRES- $\beta$ -geo cassette was inserted within the 3' untranslated sequences of the H-*Ras* gene (see Supplemental Fig. S1 for further details). This allows the expression of  $\beta$ -galactosidase in a bicistronic fashion with the wild-type or the oncogenic H-*Ras*<sup>G12V</sup> protein under the regulation of the endogenous H-*Ras* promoter. The comparison of X-gal staining in the brain of adult H-*Ras*<sup>geo/geo</sup> and H-*Ras*<sup>G12V/G12V</sup> mice revealed a similar pattern and level of expression for the H-*Ras* and H-*Ras*<sup>G12V</sup> alleles (Fig. 1), suggesting that the expression of the oncogenic H-*Ras*<sup>G12V</sup> protein did not perturb the pattern of expression of the H-*Ras* locus. Many structures of the brain showed robust X-gal staining, including the hippocampus, the cerebral cortex, the amygdala and the striatum. These areas

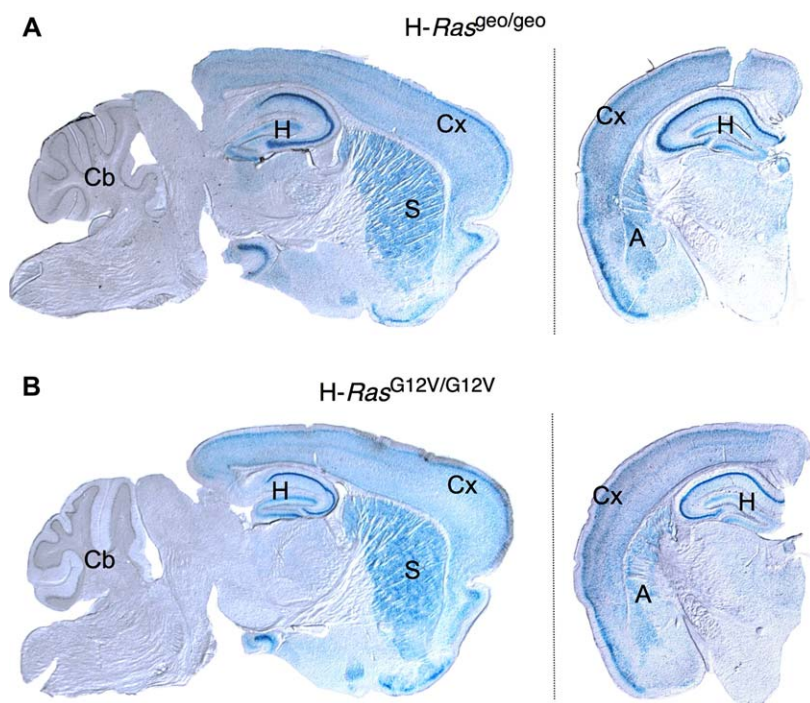


**Figure 1: Analysis of H-Ras expression in the brain of adult H-Ras<sup>geo/geo</sup> and H-Ras<sup>G12V/G12V</sup> mice.** Sagittal and coronal vibratome sections were submitted to X-gal staining to determine  $\beta$ -galactosidase activity as a surrogate marker for expression of H-Ras<sup>geo</sup> (A) and H-Ras<sup>G12V</sup> (B) alleles. Note the low level of expression in the cerebellum (Cb) compared with other brain areas, including amygdala (Ag), cortex (Cx), hippocampus (Hp) and striatum (St). No significant differences were observed in the pattern and level of expression of the H-Ras<sup>geo</sup> and H-Ras<sup>G12V</sup> alleles.

are critically involved in different forms of memory and in the control of emotional responses. In contrast, expression in the cerebellum was low. Regarding cell type, H-Ras expression was especially strong in pyramidal neurons of hippocampus and cortex. Notably, H-Ras expression was much stronger in pyramidal neurons of the CA1 and CA3 subfield than in granular neurons of the dentate gyrus (DG).

Nissl staining (results not shown) and immunohistochemistry of brain sagittal sections from H-Ras<sup>G12V/G12V</sup> mice using the neuronal markers microtubule associated protein 2 (MAP2) and synaptophysin did not reveal any obvious abnormality in brain anatomy (Fig. 2). Because cAMP response element binding protein (CREB)-mediated gene expression, downstream of Ras/Raf/Mek, has been critically involved in cognitive and emotional processes (Barco *et al.* 2003; Lonze & Ginty 2002), we examined the activation of target proteins in the CREB pathway downstream of H-Ras in the brain of H-Ras<sup>G12V/G12V</sup> mice. In agreement with previous analyses by Western blot (Schuhmacher *et al.* 2008), we did not observe dramatic changes in the level of Erk1/2 phosphorylation in the brain (results not shown), suggesting the existence of negative feedback mechanisms that compensate the chronic activation of H-Ras. More detailed observation revealed, however, local changes in the level of active Erk1/2. In particular, the mossy fibers of H-Ras<sup>G12V/G12V</sup> mice showed augmented immunoreactivity to phospho-Erk1/2 (Fig. 2). However, we did not observe changes in the number of DG granular cells, the neurons that form the mossy fiber projection, that were positive for phospho-CREB, downstream of Erk1/2, or for c-fos, an inducible transcription factor downstream of CREB (Fig. 2).

#### Gross neurological examination of CS mouse models

Children with CS show significant irritability, sleep disturbance and excess shyness (Galera *et al.* 2006; Kawame *et al.* 2003). To verify whether H-Ras<sup>G12V</sup> mutant mice show similar neurological and behavioral defects, we subjected them to a comprehensive battery of basal neurological tests (Irwin 1968; Rogers *et al.* 1997). Both, hetero and homozygous H-Ras<sup>G12V</sup> mice had normal size, weight and proportioned overall dimensions (Table 1). Mutant mice were sometimes distinguished because they displayed facial dysmorphia and engrossed lips (Schuhmacher *et al.* 2008), two phenotypes that are reminiscent of the distinctive facial appearance of CS patients (Hennekam 2003). No differences were observed in basic reflexes, strength, muscle tone and other parameters evaluated in this primary screening neither in heterozygous nor homozygous mutants (Table 1). We also found no differences between the two genotypes and their littermates in an accelerated Rotarod paradigm, a task that evaluates motor coordination and learning, and in the hot plate, a test to measure nociception and sensitivity to thermal stimulus (Table 1). H-Ras<sup>+G12V</sup> and wild-type littermates also showed similar startle response (Supplemental Fig. S2A:  $F_{(1,15)}^{\text{genotype}} = 0.244$ ,  $P = 0.628$ ;  $F_{(8,20)}^{\text{pulse} \times \text{genotype}} = 0.715$ ,  $P = 0.678$ ;  $F_{(8,20)}^{\text{pulse}} = 17.487$ ,  $P < 0.001$ ). PPI, a classical test for sensorimotor gating was also unaltered in H-Ras<sup>+G12V</sup> mice (Supplemental Fig. S2B:  $F_{(1,22)}^{\text{genotype}} = 0.501$ ,  $P = 0.487$ ;  $F_{(2,44)}^{\text{pp} \times \text{genotype}} = 1.671$ ,  $P = 0.200$ ;  $F_{(2,44)}^{\text{pp}} = 16.603$ ,  $P < 0.001$ ). In conclusion, H-Ras<sup>G12V</sup> mice did not show any abnormality in neurological function that prevented or confounded the interpretation of further behavioral analyses.

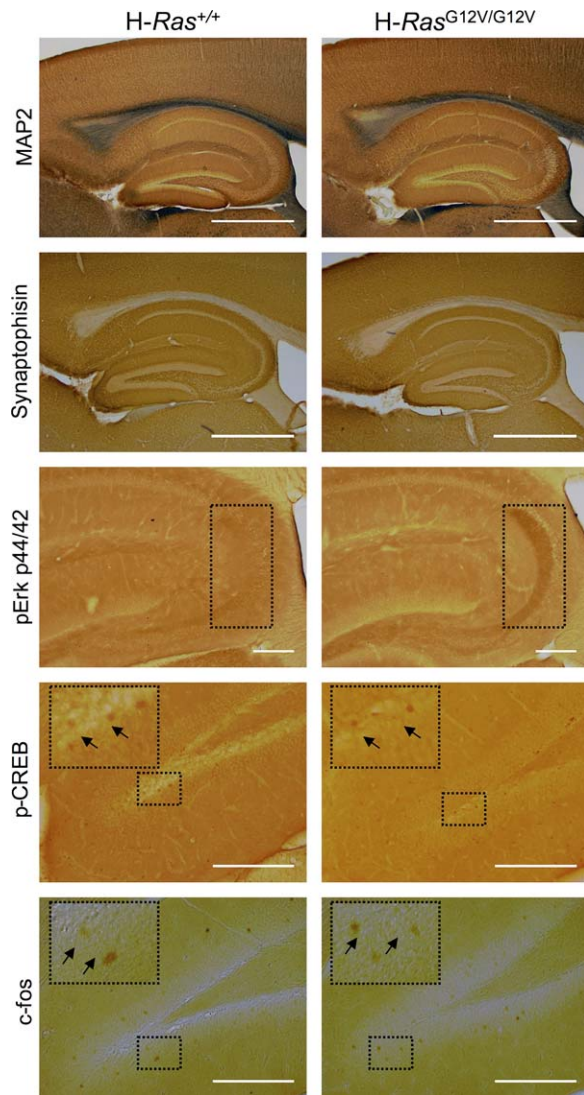


**Figure 2: Immunohistochemical analysis of H-Ras<sup>G12V/G12V</sup> mice.** Floating vibratome sections (50  $\mu$ M) were stained with antibodies against MAP2, synaptophysin, phospho-Erk1/2, phospho-CREB and c-fos. As expected, the immunostaining for phospho-CREB and c-fos was very weak except for a few scattered cells. This analysis did not reveal significant differences between genotypes, with the exception of enhanced phospho-Erk1/2 staining in the mossy fiber of H-Ras<sup>G12V/G12V</sup> mice (dashed square). No differences in phospho-CREB and c-fos immunostaining (see arrows in higher magnification inset) were observed in the granular layer. Similar results were obtained in three different H-Ras<sup>G12V/G12V</sup> mice and their control littermates. Scale bars: 1 mm for MAP2 and synaptophysin, 200  $\mu$ m for phospho-Erk1/2, phospho-CREB and c-fos.

### General activity and anxiety-like phenotype in CS mouse models

We investigated the general activity of H-Ras<sup>G12V</sup> mice in an open field for 30 min (Fig. 3 and Supplemental Fig. S2). Heterozygous mice (top panels) showed normal locomotor

activity (Fig. 3A), whereas homozygous mice exhibited reduced activity in the novel environment. Hypolocomotion was evidenced in both the reduced ambulatory distance (Fig. 3C:  $F_{(1,15)\text{genotype}} = 8.78$ ,  $P = 0.010$ ) and the enhanced resting time (Supplemental Fig. S3A:  $F_{(1,15)\text{genotype}} = 9.347$ ,  $P = 0.008$ ). No significant change in ambulatory or maximum speed was found in either genotype (Supplemental Fig. S3A). This analysis also detected subtle, but statistically significant differences in the time spent by H-Ras<sup>+/G12V</sup> mice in the center of the arena, a common measure of anxiety (Fig. 3B:  $F_{(1,20)\text{genotype}} = 4.657$ ,  $P = 0.043$ ). No significant difference was observed for this parameter in homozygous mice (Fig. 3D).

To further explore anxiety and evaluate whether these mouse strains could represent a useful model to investigate the hypermotivity associated to CS, we examined the performance of H-Ras<sup>G12V</sup> mice in the elevated plus maze, a task in which mice face a conflict between their tendency to explore new environments and their innate aversion to open, brightly light spaces. Both hetero and homozygous mutants showed a reduced number of arm entries in the elevated plus maze (Fig. 4A: H-Ras<sup>+/G12V</sup>  $t_{20} = 3.066$ ,  $P = 0.006$ ; Fig. 4C: H-Ras<sup>G12V/G12V</sup>  $F_{(1,17)\text{genotype}} = 10.827$ ,  $P = 0.004$ ). In addition, homozygous mice, but not heterozygous mice (Fig. 4B), spent less time in the open arms (Fig. 4D:  $F_{(1,17)\text{genotype}} = 5.274$ ,  $P = 0.035$ ). Taken together, these observations indicate that H-Ras<sup>G12V</sup> mice have higher anxiety than wild-type animals, a phenotype that could be gene dose dependent because the differences were especially significant in homozygous mutants.

### Cognitive impairments in CS mouse models

CS patients display mild to borderline mental retardation (Hennekam 2003). To assess cognitive impairments in H-Ras<sup>G12V</sup> mutant mice, we tested these mutants in several learning and memory tasks. We examined the performance of H-Ras<sup>G12V</sup> mice in spatial navigation using the MWM. We divided this task in three phases starting with the visible platform version of the task to evaluate vision, motivation and swimming performance. Then, we examined spatial learning using the hidden platform version of the water maze for eight days and assessed spatial memory performing probe trials on days 5 and 9. We concluded the MWM experiment assessing learning flexibility by transferring the platform to a new position, training for 5 additional days and performing a final probe trial on day 6 of transfer.

Both, homo and heterozygous mutants performed well in the visible platform task and did not show differences in escape path length (Fig. 5A:  $F_{(1,19)\text{genotype}} = 0.006$ ,  $P = 0.941$ ,  $F_{(2,38)\text{genotype} \times \text{session}} = 0.061$ ,  $P = 0.941$ ; Fig. 5B:  $F_{(1,17)\text{genotype}} = 0.0611$ ,  $P = 0.809$ ,  $F_{(2,34)\text{genotype} \times \text{session}} = 1.059$ ,  $P = 0.358$ ), and swimming speed (Supplemental Fig. S4A: H-Ras<sup>+/G12V</sup>  $F_{(1,19)\text{genotype}} = 2.694$ ,  $P = 0.117$ ,  $F_{(2,38)\text{genotype} \times \text{session}} = 1.398$ ,  $P = 0.260$ ; H-Ras<sup>G12V/G12V</sup>  $F_{(1,17)\text{genotype}} = 0.027$ ,  $P = 0.871$ ,  $F_{(2,34)\text{genotype} \times \text{session}} = 1.237$ ,  $P = 0.303$ ).

In the hidden platform task, H-Ras<sup>+/G12V</sup> mice did not show any deficit either (Fig. 5A:  $F_{(1,19)\text{genotype}} = 0.874$ ,  $P = 0.362$ ;  $F_{(7,133)\text{genotype} \times \text{session}} = 0.625$ ,  $P = 0.734$ ), but

**Table 1:** Basal behavior analysis of H-Ras<sup>+/G12V</sup> and H-Ras<sup>G12V/G12V</sup> mice

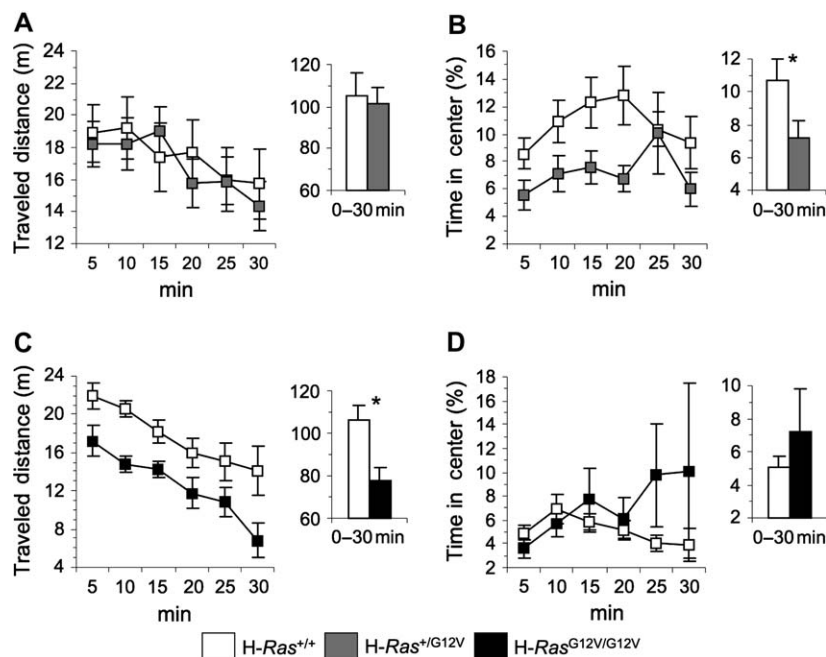
	H-Ras <sup>+/G12V</sup>				H-Ras <sup>G12V/G12V</sup>			
	+ /+	+ /G12V	Statistic	P value	+ /+	G12V/G12V	Statistic	P value
Behavioral primary screen								
Abdominal tone	1 (1–1)	1 (1–1)	<i>U</i> = 55	ns	1 (1–1)	1 (1–1)	<i>U</i> = 18	ns
Body length(mm)	87 (85–89)	89 (83–90)	<i>U</i> = 50.5	ns	98 (94.5–100)	95 (93–97)	<i>U</i> = 9.5	ns
Body position	3 (3–3)	3 (2–3)	<i>U</i> = 49.5	ns	3 (3–3)	3 (2–3)	<i>U</i> = 12	ns
Contact righting reflex	1 (1–1)	1 (1–1)	<i>U</i> = 60.5	ns	1 (1–1)	1 (1–1)	<i>U</i> = 18	ns
Corneal reflex	1 (1–1)	1 (1–1)	<i>U</i> = 60.5	ns	1 (1–1)	1 (1–1)	<i>U</i> = 18	ns
Defecation	3 (1–4)	2 (1.75–2.25)	<i>U</i> = 36	ns	3 (2.5–4.25)	2.5 (1.75–4)	<i>U</i> = 14	ns
Fear	0 (0–0)	0 (0–0)	<i>U</i> = 60.5	ns	0 (0–0.25)	0 (0–0)	<i>U</i> = 15	ns
Gait	0 (0–0)	0 (0–0)	<i>U</i> = 55	ns	0 (0–0)	0 (0–0.25)	<i>U</i> = 15	ns
Grip strength	3 (3–3)	3 (2–3)	<i>U</i> = 49.5	ns	3 (3–3)	3 (2.75–3)	<i>U</i> = 15	ns
Irritability	1 (1–1)	1 (1–1)	<i>U</i> = 55	ns	1 (1–1)	1 (1–1)	<i>U</i> = 15	ns
Lacrimation	0 (0–0)	0 (0–0)	<i>U</i> = 60.5	ns	0 (0–0)	0 (0–0)	<i>U</i> = 18	ns
Limb grasping	1 (1–1)	1 (1–1)	<i>U</i> = 60.5	ns	1 (1–1)	1 (1–1)	<i>U</i> = 18	ns
Limb tone	1 (0–1)	1 (0–1)	<i>U</i> = 55	ns	2 (2–2)	2 (2–2)	<i>U</i> = 18	ns
Locomotor activity	16.4 ± 0.8	15.4 ± 0.9	<i>t</i> <sub>(20)</sub> = -0.765	ns	12.0 ± 1.3	9.8 ± 1.6	<i>t</i> <sub>(10)</sub> = 1.03	ns
Negative geotaxis	0 (0–0)	0 (0–0)	<i>U</i> = 55	ns	0 (0–0)	0 (0–0)	<i>U</i> = 18	ns
Palpebral closure	0 (0–0)	0 (0–0)	<i>U</i> = 60.5	ns	0 (0–0)	0 (0–0)	<i>U</i> = 18	ns
Pelvic elevation	3 (3–3)	3 (3–3)	<i>U</i> = 58.5	ns	2 (2–2)	2 (2–2)	<i>U</i> = 18	ns
Piloerection	0 (0–0)	0 (0–0)	<i>U</i> = 60.5	ns	0 (0–0)	0 (0–0)	<i>U</i> = 18	ns
Pinna reflex	1 (1–1)	1 (1–1)	<i>U</i> = 60.5	ns	1 (1–1)	1 (1–1)	<i>U</i> = 15	ns
Provoked biting	1 (1–1)	1 (0–1)	<i>U</i> = 40.5	ns	0 (0–1)	1 (0.25–1)	<i>U</i> = 7	ns
Righting reflex	0 (0–0)	0 (0–0)	<i>U</i> = 60.5	ns	0 (0–0)	0 (0–0)	<i>U</i> = 18	ns
Skin color	1 (1–1)	1 (1–1)	<i>U</i> = 55	ns	2 (2–2)	2 (2–2)	<i>U</i> = 18	ns
Spontaneous activity	2 (2–2)	2 (2–2)	<i>U</i> = 56	ns	2.5 (2–3)	3 (2.75–3)	<i>U</i> = 12	ns
Tail elevation	2 (2–2)	2 (2–2)	<i>U</i> = 55	ns	1.5 (1–2)	1.5 (1–2)	<i>U</i> = 18	ns
Toe pinch	2 (2–3)	2 (2–3)	<i>U</i> = 55	ns	3 (3–3)	3 (3–3)	<i>U</i> = 12	ns
Touch escape	2 (2–2)	2 (2–2)	<i>U</i> = 49.5	ns	3 (2–3)	2.5 (2–3)	<i>U</i> = 15	ns
Transfer arousal	4 (3–4)	4 (4–4)	<i>U</i> = 58.5	ns	4 (3.75–4)	4 (4–4.25)	<i>U</i> = 12.5	ns
Tremor	0 (0–0)	0 (0–0)	<i>U</i> = 55	ns	1 (0.5–1)	1 (1–1)	<i>U</i> = 10	ns
Trunk curl	0 (0–0)	0 (0–0)	<i>U</i> = 60.5	ns	0 (0–0)	0 (0–0)	<i>U</i> = 18	ns
Urination	0 (0–0)	0 (0–0)	<i>U</i> = 49.5	ns	0 (0–0)	0 (0–0)	<i>U</i> = 18	ns
Vibrissae	0 (0–1)	0 (0–1)	<i>U</i> = 60.5	ns	0 (0–0.25)	0 (0–0)	<i>U</i> = 15	ns
Visual placing	2 (2–2)	2 (2–2)	<i>U</i> = 60.5	ns	3 (2.5–3)	3 (3–3)	<i>U</i> = 15	ns
Vocalization	1 (1–1)	1 (1–1)	<i>U</i> = 60.5	ns	0.5 (0–1)	0.5 (0–1)	<i>U</i> = 18	ns
Weight (g)	25.3 ± 0.7	26.3 ± 0.7	<i>t</i> <sub>(20)</sub> = 1.002	ns	28.1 ± 1.7	24.8 ± 1.7	<i>t</i> <sub>(10)</sub> = 1.357	ns
Wire maneuver	2 (2–2)	2 (2–2)	<i>U</i> = 45	ns	1 (0.75–2.25)	1 (0–1)	<i>U</i> = 11	ns
Hot plate								
Latency	8.90 ± 1.03	8.02 ± 0.53	<i>t</i> <sub>(22)</sub> = 0.827	ns	10.1 ± 0.9	9.4 ± 0.7	<i>F</i> <sub>(1,17)</sub> = 0.307	ns
Rotarod								
Latency to fall (s)	123.2 ± 9.4	100.8 ± 16.8	<i>t</i> <sub>(20)</sub> = 1.158	ns	114.6 ± 23.8	102.4 ± 14.7	<i>F</i> <sub>(1,15)</sub> = 0.166	ns

No gross neurological abnormalities in heterozygous or homozygous mice were revealed in a primary screen (H-Ras<sup>+/G12V</sup> and littermates, *n* = 11 for both genotypes; H-Ras<sup>G12V/G12V</sup> and littermates, *n* = 6 for both genotypes). Nociceptive perception (H-Ras<sup>+/G12V</sup> and littermates, *n* = 14, 10; H-Ras<sup>G12V/G12V</sup> and littermates, *n* = 11, 10) and motor coordination were also unaffected (H-Ras<sup>+/G12V</sup> and littermates, *n* = 11, 11; H-Ras<sup>G12V/G12V</sup> and littermates, *n* = 10, 9). *P* values are calculated using *t*-test or ANOVA for data expressed as mean ± SEM, and Mann–Whitney test for data expressed as median followed by interquartile range.

H-Ras<sup>G12V/G12V</sup> mice exhibited significant impairments as shown in the escape path length learning curve (Fig. 5B: *F*<sub>(1,17)genotype</sub> = 6.923, *P* = 0.018; *F*<sub>(7,119)genotype×session</sub> = 0.223, *P* = 0.979). In agreement with these results, homozygous mice had memory deficits in the first probe trial. There

was a significant quadrant × genotype interaction for the percentage of time spent in the different quadrants (*F*<sub>(3,51)</sub> = 3.317, *P* = 0.027) and an almost significant interaction for the annulus crossings (*F*<sub>(3,51)</sub> = 2.607, *P* = 0.062). Moreover, the analysis of annulus crossings revealed that homozygous mice

**Figure 3: Open field activity in H-*Ras*<sup>G12V</sup> mice.** Mice were placed in an open field and monitored for 30 min using a videotracking system. Traveled distance (A, C) and percentage of time spent in the center of the arena (B, D) were calculated in time bins of 5 min (line graphs) and for the whole 30-min period (bar graph insets). (A, B) H-*Ras*<sup>+G12V</sup> mice ( $n = 11$ ) and wild-type littermates ( $n = 11$ ) traveled similar distances, but H-*Ras*<sup>+G12V</sup> mice spent less time in the center of the arena. (C, D) H-*Ras*<sup>G12V/G12V</sup> mice ( $n = 9$ ) showed reduced exploration than their wild-type littermates ( $n = 10$ ). Asterisks indicate statistical significance ( $P < 0.05$ ). See Supplemental Fig. S3 for additional information on locomotor and exploratory activity.



failed to show a preference for the target quadrant (Fig. 5D:  $t_{(10)} = 1.564$ ,  $P = 0.149$ ), whereas their wild-type littermates showed strong preference (Fig. 5D:  $t_{(9)} = 3.511$ ,  $P = 0.007$ ). The analyses of quadrant occupancy also revealed this memory deficit. H-*Ras*<sup>G12V/G12V</sup> mice did not show a preference for the target quadrant when compared to the chance value of 25% (Supplemental Fig. S4C:  $t_{(10)} = 1.924$ ,  $P = 0.083$ ), whereas control littermates showed a strong preference (Supplemental Fig. S4C:  $t_{(9)} = 5.324$ ,  $P < 0.001$ ). The comparison between genotypes revealed almost significant difference ( $F_{(1,17)} \text{genotype} = 4.152$ ,  $P = 0.057$ ). No deficit was observed in P2 and P3, indicating that the memory impairment of homozygous mice was compensated with further training.

Finally, in the transfer task, neither H-*Ras*<sup>+G12V</sup> mice nor H-*Ras*<sup>G12V/G12V</sup> mice showed significant defects (Fig. 5A:  $F_{(1,19)} \text{genotype} = 0.277$ ,  $P = 0.604$ ;  $F_{(4,76)} \text{genotype} \times \text{session} = 0.214$ ,  $P = 0.084$ ; Fig. 5B:  $F_{(1,17)} \text{genotype} = 2.552$ ,  $P = 0.129$ ;  $F_{(4,68)} \text{genotype} \times \text{session} = 1.174$ ,  $P = 0.330$ ). This result suggests that the learning delay observed for homozygous mice in the hidden platform task can also be overcome with further training in the water maze.

Notably, homozygous mice showed higher level of thigmotaxis than their control littermates in the hidden platform task (Fig. 5C:  $F_{(1,17)} \text{genotype} = 7.754$ ,  $P = 0.013$ ;  $F_{(7,119)} \text{genotype} \times \text{session} = 0.995$ ,  $P = 0.438$ ), but not in the visible platform (Fig. 5C:  $F_{(1,17)} \text{genotype} = 1.203$ ,  $P = 0.288$ ,  $F_{(2,34)} \text{genotype} \times \text{session} = 1.015$ ,  $P = 0.373$ ), and the transfer task (Fig. 5C:  $F_{(1,17)} \text{genotype} = 1.196$ ,  $P = 0.289$ ;  $F_{(4,68)} \text{genotype} \times \text{session} = 0.328$ ,  $P = 0.858$ ). The elevated thigmotaxis during the most demanding phase of this learning paradigm might be a consequence of the enhanced anxiety observed in these mice (Fig. 4). This trait was not observed in heterozygous mice (Supplemental Fig. S4B:  $F_{(1,19)} \text{genotype} = 2.94$ ,  $P = 0.103$ ,

$F_{(2,38)} \text{genotype} \times \text{session} = 2.123$ ,  $P = 0.134$ ), supporting again the notion of a gene dose effect in anxiety-like phenotypes.

We also trained H-*Ras*<sup>G12V</sup> mice in an object recognition memory task, a non aversive memory task that relies on the natural exploratory behavior of mice. We assessed recognition memory retention 24 h after training. The experiments did not reveal significant differences between hetero- and homozygous mice, and their respective control littermates (Fig. 6A, test session: H-*Ras*<sup>+G12V</sup>  $t_{(20)} = 1.117$ ,  $P = 0.277$ ; H-*Ras*<sup>G12V/G12V</sup>  $F_{(1,17)} \text{genotype} = 0.010$ ,  $P = 0.922$ ). Despite the lower activity observed in the open field task, homozygous mice and wild-type littermates spent a similar percentage of time investigating the objects (Supplemental Fig. S5:  $F_{(1,17)} \text{genotype} = 2.133$ ,  $P = 0.162$ ;  $F_{(1,17)} \text{genotype} \times \text{session} = 1.377$ ,  $P = 0.257$ ). Heterozygous mice also showed normal exploratory activity (Supplemental Fig. S5:  $F_{(1,20)} \text{genotype} = 1.360$ ,  $P = 0.257$ ;  $F_{(1,20)} \text{genotype} \times \text{session} = 0.010$ ,  $P = 0.920$ ).

We concluded our battery of cognitive tasks by testing contextual fear conditioning. This task measures the capability of the mouse to form an association between an aversive stimulus and neutral environmental context. We found that H-*Ras*<sup>G12V</sup> mice and wild-type littermates exhibited similar memory for this task (Fig. 6B). Interestingly, we observed a significant difference in the immediate freezing response to the shock in both mutant genotypes (Fig. 6C: H-*Ras*<sup>+G12V</sup>  $t_{(20)} = 2.996$ ,  $P = 0.007$ ; H-*Ras*<sup>G12V/G12V</sup>  $F_{(1,16)} \text{genotype} = 6.246$ ,  $P = 0.024$ ), a phenotype not related to memory, but that suggest again an enhanced emotivity.

## Discussion

CS is a rare congenital condition caused by germline expression of constitutively active/oncogenic alleles of H-RAS. To

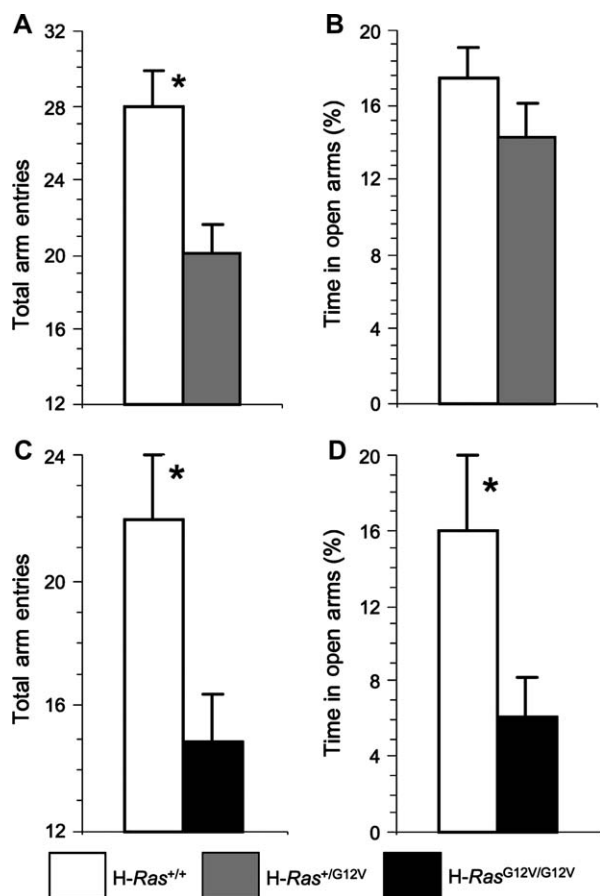


**Figure 4: Elevated anxiety in adult H-Ras mutant mice.** (A) H-Ras<sup>+/G12V</sup> mice ( $n = 11$ ) showed a lower number of arm entries than wild-type littermates ( $n = 11$ ). (B) H-Ras<sup>+/G12V</sup> and control mice spent similar percentage of time in the open arms. (C) H-Ras<sup>G12V/G12V</sup> mice ( $n = 11$ ) also showed a lower number of arm entries than their control littermates ( $n = 10$ ). (D) H-Ras<sup>G12V/G12V</sup> mice spent less time than control littermates in the open arms. Asterisks indicate statistical significance ( $P < 0.05$ ).

better understand this disease, Schuhmacher *et al.* generated a genetically equivalent mouse model by knocking-in one of the CS mutations (G12V) within the endogenous mouse H-Ras locus. These mice closely phenocopied some of the defects observed in CS patients (Schuhmacher *et al.*, 2008). The neurological and behavioral analysis of H-Ras<sup>G12V</sup> mice indicates that these animals could also be used to model some aspects of the hyperemotivity and hypersensibility observed in children with CS. We have shown that H-Ras<sup>G12V</sup> mice have higher anxiety and emotivity levels than wild-type animals and revealed mild cognitive deficits in the case of homozygous mice. Both phenotypes are reminiscent of the neurological traits observed in CS patients.

More precisely, we found that H-Ras<sup>G12V</sup> heterozygous mice showed increased avoidance toward open spaces and enhanced conditioned freezing. H-Ras<sup>G12V</sup> homozygous mice also showed the second phenotype and, in addition, exhibited

enhanced thigmotaxis in the hidden platform task and increased avoidance of the open arms in the elevated plus maze. Homozygous mice showed hypolocomotion in three different environments: open field arena (Fig. 3), elevated plus maze (Fig. 4) and *IntelliCage* (Supplemental Fig. S3B). Hypolocomotion could be a consequence of the enhanced anxiety, because we did not detect motor impairments in the modified SHIRPA screen and the Rotarod task (Table 1), or reduced swimming speed in water maze tasks (Supplementary Fig. S4A). Thus, anxiety-like behavioral traits seem to be especially marked in homozygous mutants, suggesting the existence of a gene dose effect that was also manifested in the cardiovascular phenotype (Schuhmacher *et al.* 2008). However, we should note that we have only compared homozygous and heterozygous mice with their respective wild-type littermates. The analysis of a cohort of mice including both homozygous and heterozygous littermates would enable the direct comparison between genotypes and would further support a gene dose effect on anxiety-like phenotypes.

Our study also revealed cognitive impairments that may resemble the mild cognitive and memory deficits observed in CS patients (Axelrad *et al.* 2007). Homozygous mutant showed significantly larger escape path lengths and latencies to reach the platform in the hidden platform task, as well as memory impairments in the first probe trial for this task. Mild cognitive impairments were manifested in the water maze, but not in the contextual fear and object recognition memory tasks, and were only found in homozygous mice, suggesting that to model the borderline mental retardation observed in most CS patients it is necessary to exacerbate the underlying molecular alteration. In agreement with the indirect evidence for a gene dose effect found in H-Ras<sup>G12V</sup> mice, recent observations indicate that the degree of cognitive impairment in CS patients might correlate to the degree of gain-of-function conveyed by the germline mutation (Axelrad *et al.* 2007).

Impaired spatial learning and altered emotivity are difficult to dissociate in H-Ras<sup>G12V/G12V</sup> mice. Anxiety-related thigmotactic behavior correlated with learning impairments and might significantly contribute to the observed learning delays. Interestingly, enhanced thigmotaxis was only observed in the hidden platform task, which might suggest that anxiety-like behaviors were stressed when the mice were challenged with a novel, and more demanding, cognitive task. Once the mice adapted to the absence of the visual cue that labeled the platform location, thigmotactic behavior was ameliorated with training. The normal level of thigmotaxis during the transfer task and the compensation of the initial memory defect observed in the second and third probe trial support this interpretation. Similarly to this mouse model, altered emotivity and sensibility may importantly contribute to the feeding problem, failure to thrive and delayed learning observed in children with CS (Richter & Bradley 1996).

The signaling pathway altered in CS mice has been critically involved in neuronal stress, anxiety, learning and memory in the mature brain (Barco *et al.* 2006; Lonze & Ginty 2002; Thomas & Haganir 2004), it is therefore possible that some of the neurological abnormalities observed in children with CS may not simply be because of defects originated during

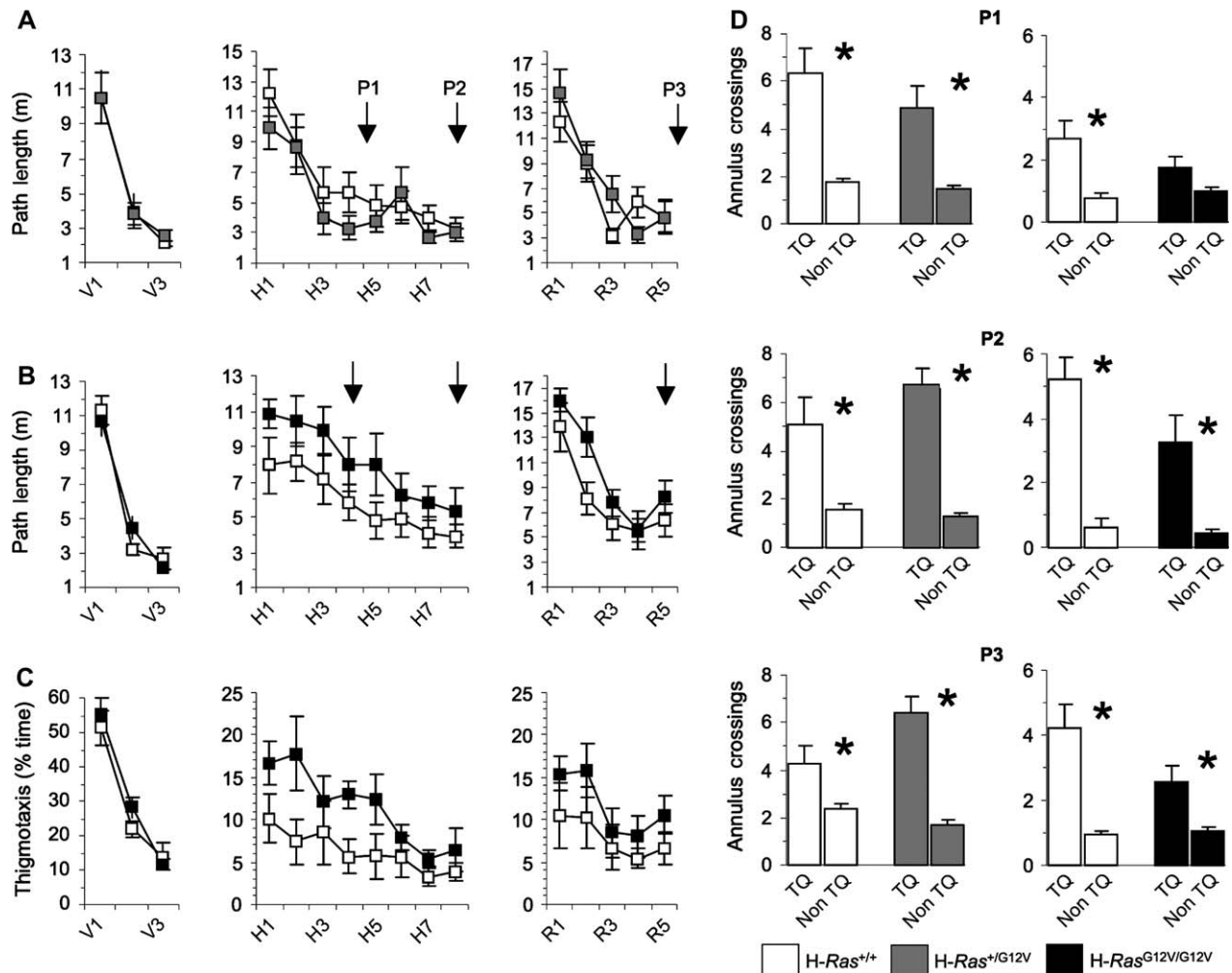


**Figure 5: Spatial navigation and memory in *H-Ras*<sup>G12V</sup> mice.** (A) *H-Ras*<sup>+G12V</sup> mice ( $n = 11$ ) and control littermates ( $n = 10$ ) behave similarly in the visible and hidden platform tasks. These mice also behave similarly when learning a new position of the platform (transfer task). (B) *H-Ras*<sup>G12V/G12V</sup> mice ( $n = 11$ ) and control littermates ( $n = 10$ ) behave similarly in the visible platform tasks, but showed significant impairments in the hidden platform task that disappeared in the transfer task. (C) *H-Ras*<sup>G12V/G12V</sup> exhibit significantly higher level of thigmotaxis than control siblings during training in the hidden platform task, but not in the visible or the transfer tasks. (D) No significant differences were observed in heterozygous mice when spatial memory was assessed in three probe trials. In all cases, mutant mice showed a good memory for the platform location (asterisks indicate  $P < 0.05$ ). In homozygous mice, we observed an initial memory deficit (no significant difference between the TQ and the other quadrants in the first probe trial) that disappeared with further training. See Supplemental Fig. S4 for additional information.

development of the nervous system, but result from the chronic abnormal activity of this signaling pathway throughout life. Surprisingly, the recent analysis of transgenic mice expressing postnatally in a restricted manner the same activating mutation investigated here, *H-Ras*<sup>G12V</sup>, revealed strong activation of downstream targets and enhanced learning and memory (Kushner *et al.* 2005) that contrast with the cognitive impairments and behavioral deficits observed in knock-in mice and in CS patients. These results suggest that the pattern and time of expression of the mutation has a critical impact on its consequences on behavior. The analysis of inducible and brain restricted *H-*

*Ras*<sup>G12V</sup> mutant mice may allow to further dissect the specific effects of the mutation during development and in adulthood. Those studies should have a significant impact on our understanding and treatment of neurological traits associated to CS.

The availability of animal models for CS will help to develop potential therapeutic strategies for this rare disease. Thus, the cardiovascular deficits observed in CS mice were associated to abnormal upregulation of the rennin–Ang II system; Schuhmacher *et al.* (2008) successfully prevented development of the hypertension condition, vascular remodeling, and heart and kidney fibrosis by treating the mice with captopril,

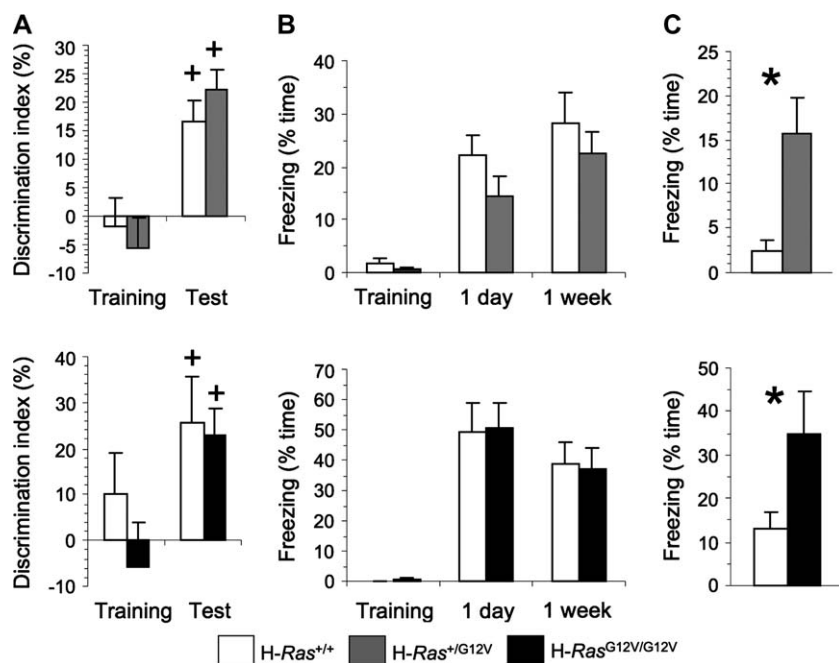


**Figure 6: Novel Object recognition and fear conditioning memory in H-Ras<sup>G12V</sup> mutant mice.** (A) Normal object recognition memory 24 h after training. Both mutant strains and their corresponding wild-type littermates did not show significant preference for either object during training, but explored more the novel object during the testing session (+: significantly different from the chance value 0%). The groups analyzed included 11 H-Ras<sup>+/G12V</sup> mice and 11 wild-type littermates, and 11 H-Ras<sup>G12V/G12V</sup> and 10 wild-type littermates. See Supplemental Fig. S5 for additional information. (B) Contextual fear conditioning in H-Ras<sup>G12V</sup> mice. Mice were tested 24 h and 7 days after training. In both cases we did not observe any difference in mutant mice when compared to their respective wild-type littermates. The groups analyzed included 11 H-Ras<sup>+/G12V</sup> mice and 11 wild-type littermates, and 11 H-Ras<sup>G12V/G12V</sup> and 9 wild-type littermates. (C) Both H-Ras<sup>+/G12V</sup> and H-Ras<sup>G12V/G12V</sup> mice showed more freezing immediately after the shock (conditioned freezing) than wild-type littermates. Asterisks indicate statistical significance ( $P < 0.05$ ).

an inhibitor of Ang II biosynthesis. These animals could be also used to test whether inhibitors of H-Ras farnesylation or downstream targets, such as the Raf/Mek pathway and the PI3K/Akt route, have therapeutic value.

We did not observe gross abnormalities in the level of some putative H-Ras targets, such as phospho-Erk1/2 and phospho-CREB, suggesting that neurons may have efficient negative regulatory feedback mechanisms that prevent excessive Ras signaling. However, we observed locally restricted alterations in phospho-Erk1/2 immunoreactivity at the mossy fiber projection of H-Ras<sup>G12V/G12V</sup> mice despite of clearly lower expression of H-Ras in granular cells of the DG than in other neuronal populations (Fig. 1). Although at this time such phenotype is difficult to interpret, hyperphosphorylation of Erk1/2 may reflect or cause enhanced activity in this pathway. Interestingly, a recent study correlated enhanced activity at the mossy fibers with increase in anxiety-like behavior in rats (Takeda et al. 2008), suggesting that both phenotypes may be linked. In conclusion, although the specific molecular alterations downstream of H-Ras that underlay the phenotype of H-Ras<sup>G12V</sup> mice remain unknown (Schuhmacher et al. 2008), the neurological defects observed in CS patients and H-Ras<sup>G12V</sup> mice indicate that abnormal Ras signaling by CS mutations have important consequences

on the development and/or function of neuronal circuits underlying anxiety and cognition.

## References

- Aoki, Y., Niihori, T., Kawame, H., Kurosawa, K., Ohashi, H., Tanaka, Y., Filocamo, M., Kato, K., Suzuki, Y., Kure, S. & Matsubara, Y. (2005) Germline mutations in HRAS proto-oncogene cause Costello syndrome. *Nat Genet* **37**, 1038–1040.
- Aoki, Y., Niihori, T., Narumi, Y., Kure, S. & Matsubara, Y. (2008) The RAS/MAPK syndromes: novel roles of the RAS pathway in human genetic disorders. *Hum Mutat* **29**, 992–1006.
- Axelrad, M.E., Glidden, R., Nicholson, L. & Gripp, K.W. (2004) Adaptive skills, cognitive, and behavioral characteristics of Costello syndrome. *Am J Med Genet A* **128**, 396–400.
- Axelrad, M.E., Nicholson, L., Stabley, D.L., Sol-Church, K. & Gripp, K.W. (2007) Longitudinal assessment of cognitive characteristics in Costello syndrome. *Am J Med Genet A* **143A**, 3185–3193.
- Barco, A., Pittenger, C. & Kandel, E.R. (2003) CREB, memory enhancement and the treatment of memory disorders: promises, pitfalls and prospects. *Expert Opin Ther Targets* **7**, 101–114.
- Barco, A., Bailey, C.H. & Kandel, E.R. (2006) Common molecular mechanisms in explicit and implicit memory. *J Neurochem* **97**, 1520–1533.
- Bertola, D.R., Pereira, A.C., Brasil, A.S., Albano, L.M., Kim, C.A. & Krieger, J.E. (2007) Further evidence of genetic heterogeneity in Costello syndrome: involvement of the KRAS gene. *J Hum Genet* **52**, 521–526.

- Bourtchouladze, R., Lidge, R., Catapano, R., Stanley, J., Gossweiler, S., Romashko, D., Scott, R. & Tully, T. (2003) A mouse model of Rubinstein-Taybi syndrome: Defective long-term memory is ameliorated by inhibitors of phosphodiesterase 4. *Proc Natl Acad Sci USA* **100**, 10518–10522.
- Costello, J.M. (1971) A new syndrome. *N Z Med J* **74**, 397.
- Estep, A.L., Tidyman, W.E., Teitell, M.A., Cotter, P.D. & Rauen, K.A. (2006) HRAS mutations in Costello syndrome: detection of constitutional activating mutations in codon 12 and 13 and loss of wild-type allele in malignancy. *Am J Med Genet A* **140**, 8–16.
- Galera, C., Delrue, M.A., Goizet, C., Etchegoyhen, K., Taupiac, P., Sigaudy, S., Arveiler, B., Philip, N., Bouvard, M. & Lacombe, D. (2006) Behavioral and temperamental features of children with Costello syndrome. *Am J Med Genet A* **140**, 968–974.
- Galsworthy, M.J., Amrein, I., Kuptsov, P.A., Poletaeva, I.I., Zinn, P., Rau, A., Vyssotski, A. & Lipp, H.P. (2005) A comparison of wild-caught wood mice and bank voles in the Intellicage: assessing exploration, daily activity patterns and place learning paradigms. *Behav Brain Res* **157**, 211–217.
- Gripp, K.W., Lin, A.E., Stabley, D.L., Nicholson, L., Scott, C.I., Jr., Doyle, D., Aoki, Y., Matsubara, Y., Zackai, E.H., Lapunzina, P., Gonzalez-Meneses, A., Holbrook, J., Agresta, C.A., Gonzalez, I.L. & Sol-Church, K. (2006) HRAS mutation analysis in Costello syndrome: genotype and phenotype correlation. *Am J Med Genet A* **140**, 1–7.
- Hennekam, R.C. (2003) Costello syndrome: an overview. *Am J Med Genet* **117**, 42–48.
- Irwin, S. (1968) Comprehensive observational assessment: Ia. A systematic, quantitative procedure for assessing the behavioral and physiologic state of the mouse. *Psychopharmacologia* **13**, 222–257.
- Kawame, H., Matsui, M., Kurosawa, K., Matsuo, M., Masuno, M., Ohashi, H., Fueki, N., Aoyama, K., Miyatsuka, Y., Suzuki, K., Akatsuka, A., Ochiai, Y. & Fukushima, Y. (2003) Further delineation of the behavioral and neurologic features in Costello syndrome. *Am J Med Genet A* **118**, 8–14.
- Kerr, B., Delrue, M.A., Sigaudy, S., et al. (2006) Genotype-phenotype correlation in Costello syndrome: HRAS mutation analysis in 43 cases. *J Med Genet* **43**, 401–405.
- Kushner, S.A., Elgersma, Y., Murphy, G.G., Jaarsma, D., van Woerden, G.M., Hojjati, M.R., Cui, Y., LeBoutillier, J.C., Marrone, D.F., Choi, E.S., De Zeeuw, C.I., Petit, T.L., Pozzo-Miller, L. & Silva, A.J. (2005) Modulation of presynaptic plasticity and learning by the H-ras/extracellular signal-regulated kinase/synapsin I signaling pathway. *J Neurosci* **25**, 9721–9734.
- Lonze, B.E. & Ginty, D.D. (2002) Function and regulation of CREB family transcription factors in the nervous system. *Neuron* **35**, 605–623.
- Lopez de Armentia, M., Jancic, D., Olivares, R., Alarcon, J.M., Kandel, E.R. & Barco, A. (2007) cAMP response element-binding protein-mediated gene expression increases the intrinsic excitability of CA1 pyramidal neurons. *J Neurosci* **27**, 13909–13918.
- Malleret, G., Hen, R., Guillou, J.L., Segu, L. & Buhot, M.C. (1999) 5-HT1B receptor knock-out mice exhibit increased exploratory activity and enhanced spatial memory performance in the Morris water maze. *J Neurosci* **19**, 6157–6168.
- Rauen, K.A., Hefner, E., Carrillo, K., et al. (2008) Molecular aspects, clinical aspects and possible treatment modalities for Costello syndrome: Proceedings from the 1st International Costello Syndrome Research Symposium 2007. *Am J Med Genet A* **146A**, 1205–1217.
- Richter, J.E. & Bradley, L.C. (1996) Psychophysiological interactions in esophageal diseases. *Semin Gastrointest Dis* **7**, 169–184.
- Rogers, D.C., Fisher, E.M., Brown, S.D., Peters, J., Hunter, A.J. & Martin, J.E. (1997) Behavioral and functional analysis of mouse phenotype: SHIRPA, a proposed protocol for comprehensive phenotype assessment. *Mamm Genome* **8**, 711–713.
- Schubbert, S., Bollag, G. & Shannon, K. (2007a) Deregulated Ras signaling in developmental disorders: new tricks for an old dog. *Curr Opin Genet Dev* **17**, 15–22.
- Schubbert, S., Shannon, K. & Bollag, G. (2007b) Hyperactive Ras in developmental disorders and cancer. *Nat Rev* **7**, 295–308.
- Schuhmacher, A.J., Guerra, C., Sauzeau, V., Canamero, M., Bustelo, X.R. & Barbacid, M. (2008) A mouse model for Costello syndrome reveals an Ang II-mediated hypertensive condition. *J Clin Invest* **118**, 2169–2179.
- Takeda, A., Itoh, H., Yamada, K., Tamano, H. & Oku, N. (2008) Enhancement of hippocampal mossy fiber activity in zinc deficiency and its influence on behavior. *Biometals* **21**, 545–552.
- Thomas, G.M. & Hagan, R.L. (2004) MAPK cascade signalling and synaptic plasticity. *Nat Rev Neurosci* **5**, 173–183.
- Zenker, M., Lehmann, K., Schulz, A.L., Barth, H., Hansmann, D., Koenig, R., Korinthenberg, R., Kreiss-Nachtsheim, M., Meinecke, P., Morlot, S., Mundlos, S., Quante, A.S., Raskin, S., Schnabel, D., Wehner, L.E., Kratz, C.P., Horn, D. & Kutsche, K. (2007) Expansion of the genotypic and phenotypic spectrum in patients with KRAS germline mutations. *J Med Genet* **44**, 131–135.

## Acknowledgments

We thank Mariano Barbacid for providing the mouse strains used in this study. This work was supported by grants from the Spanish Ministry of Education and Science to A.B. (BFU2005-00286 and SAF2005-24584-E), the European Commission to A.B. (MEXT-CT-2003-509550), the Fondo de Investigación Sanitaria to C.G. (PI042124), the Autonomous Community of Madrid to C.G. (GR/SAL/0349/2004), and Fundació La Marató de TV3 and Fundació Ramón Areces to A.B. J.V. is supported by a FPI fellowship from the Generalitat Valenciana and A.J.S. is supported by a FPU fellowship from the Spanish Ministry of Education and Science. J.V. dedicates this article to Marc Ojeda, in memoriam.

## Supporting Information

Additional Supporting Information may be found in the online version of this article.

**Figure S1:** Summary of the genetically modified H-Ras alleles used in this study. The wild-type H-Ras allele (H-Ras<sup>+</sup>) is also included for comparison. Black boxes: H-Ras coding sequences labeled with the corresponding exon number; white boxes: H-Ras noncoding exons; gray boxes: polyadenylation sequences; dotted boxes: IRES-β-geo cassette; checkered box: PGK-Hygromycin (Hyg) resistance cassette; octagonal box (STOP): transcriptional inhibitory sequences; filled triangles: loxP sites. Asterisk: G12V oncogenic mutation. LSL: loxP-STOP-loxP cassette. The proteins expressed by each allele are indicated in the right column. H-Ras<sup>G12V</sup> allele results from crossing H-Ras<sup>+ /LSL<sup>G12V</sup></sup> mice to EllaCre transgenic animals to excise the PGK-Hyg-STOP cassette flanked by loxP sites.

**Figure S2:** Acoustic startle response and PPI in H-Ras<sup>+ /G12V</sup> mice. (A) Normal startle response profile to a variety of acoustic intensities in H-Ras<sup>+ /G12V</sup> mice (n = 10) and control siblings (n = 7). Startle reflex, defined as a response significantly different from the response to background noise, was detected for intensities higher than 100 dB. (B) PPI of startle response in H-Ras<sup>+ /G12V</sup> (n = 14) and H-Ras<sup>+/+</sup> mice (n = 10). Only the 90 dB stimulus produced significant PPI (%pp90 against 0: H-Ras<sup>+/+</sup>, t<sub>(9)</sub> = 3.392, P = 0.008; H-Ras<sup>+ /G12V</sup>, t<sub>(13)</sub> = 2.419, P = 0.031). No significant effect of genotype or genotype × prepulse interaction was found.

**Figure S3:** Supplemental information on locomotor and exploratory activity in H-Ras<sup>G12V</sup> mice. (A) Open field task: Resting time, average speed and maximum speed were normal in heterozygous mice (upper panels, H-Ras<sup>+ /G12V</sup>; n = 11, H-Ras<sup>+/+</sup>; n = 11). Homozygous mice rested more time, but had similar average and maximum speed than

wild-type littermates (lower panels, H-*Ras*<sup>G12V/G12V</sup>:  $n = 9$ , H2 *Ras*<sup>+/+</sup>:  $n = 10$ ). (B) Locomotor and exploratory activity was also assessed using the automatic system IntelliCage for a period of 72 h. Both heterozygous and homozygous mice exhibited more activity during the dark phase of the light cycle ( $F_{(5,95)} \text{ phase} = 11.915$ ,  $P < 0.001$  and  $F_{(5,50)} \text{ phase} = 20.111$ ,  $P < 0.001$ , respectively). We did not observe difference in the number of visit in heterozygous mice compared to their control littermates, but, in agreement with our observations in the open field, homozygous mice showed a lower number of visits than their wild-type siblings (lower panel:  $F_{(1,10)\text{genotype}} = 11.267$ ,  $P = 0.007$ ). It should be noted that homozygous mice and littermates were tested in the IntelliCage shortly after concluding the battery of cognitive tasks, which included the highly stressful fear conditioning task. This may explain the overall lower activity of this cohort of mice in this novel environment, especially during the first day. In subsequent days the control siblings increased their activity to a level similar to that observed on the experiments on naïve animals (see upper panel), but homozygous mice still presented a low number of visits.

**Figure S4:** Supplemental information on water maze experiments. (A) No difference in average swimming speed during the three phases of the water maze experiment was found between heterozygous (upper panels) and homozy-

gous mice (lower panels) and their respective control littermates. (B) Thigmotaxis in heterozygous mice was not different from control values. (C) The analysis of quadrant occupancy during the three probe trials confirmed the normal performance of heterozygous mice and revealed a reduced preference for the target quadrant in homozygous mice during the first probe trial. In agreement with the results for annulus crossings presented in Fig. 5, in the first probe trial there was a significant quadrant  $\times$  genotype interaction for the percentage of time spent in quadrants ( $F_{(3,51)} = 3.317$ ,  $P = 0.027$ ), and an almost significant effect of genotype in the percentage of time spent in the target quadrant wild-type mice showed a significant preference for the target quadrant ( $t_{(9)} = 5.324$ ,  $P < 0.001$ ), but mutant mice did not ( $t_{(10)} = 1.924$ ,  $P = 0.083$ ). (+): significantly different from chance level (25%).

**Figure S5:** Supplemental information on object recognition memory experiments. H-*Ras*<sup>+/G12V</sup> ( $n = 11$ ) and in H-*Ras*<sup>G12V/G12V</sup> mice ( $n = 11$ ) spent similar time exploring the objects than their respective wild-type siblings ( $n = 11$  and  $n = 10$ ) both during the training and the test session.

Please note: Wiley–Blackwell are not responsible for the content or functionality of any supporting information supplied by the authors. Any queries (other than missing material) should be directed to the corresponding author.